**Geomechanics and Engineering**, *Vol. 16, No. 6 (2018) 619-626*
DOI: https://doi.org/10.12989/gae.2018.16.6.619



# A simple prediction procedure of strain-softening surrounding rock for a circular opening

Feng Wang and Jin-Feng Zou*

*School of Civil Engineering, Central South University, No.22, Shaoshan South Road, Central South University Railway Campus, Changsha, Hunan Province, 410075, People's Republic of China*

*(Received June 8, 2017, Revised November 7, 2018, Accepted November 8, 2018)*

**Abstract.** A simple prediction procedure was investigated for calculating the stresses and displacements of a circular opening. Unlike existed approaches, the proposed approach starts each step with a radius increment. The stress for each annulus could be obtained analytically, while strain increments for each step can be determinate numerically from the compatility equation by finite difference approximation, flow rule and Hooke's law. In the successive manner, the distributions of stresses and displacements could be found. It should be noted that the finial radial stress and displacement were equal to the internal supporting pressure and deformation at the tunnel wall, respectively. By assuming different plastic radii, GRC and the evolution curve of plastic radii and internal supporting pressures could be obtained conveniently. Then the real plastic radius can be calculated by using linear interpolation in the evolution curve. Some numerical and engineering examples were performed to demonstrate the accuracy and validity for the proposed procedure. The comparisons results show that the proposed procedure was faster than that in Lee and Pietrucszczak (2008). The influence of annulus number and dilation on the accuracy of solutions was also investigated. Results show that the larger the annulus number was, the more accurate the solutions were. Solutions in Park *et al.* (2008) were significantly influenced by dilation.

**Keywords:** new prediction procedure; strain-softening; circular opening; stress and displacement; GRC

## 1. Introduction

Analysis of stresses and displacements is important when a circular opening is excavated in isotropic rock masses. The distributions of stress and displacement provide reference for tunnel design. The problem can be regarded as axisymmetric and the solutions can be solved based on the Mohr-Coulomb (M-C), Hoek-Brown (H-B) and generalized H-B criteria with the elastic-perfectly plastic, elastic-brittle-plastic and strain-softening models as well as associated or non-associated flow rule, respectively. Many researchers have focused on this aspect and have made great contributions and solved many engineering problems (e.g., Antonio 2016, Apostolos 2017, Alessandra *et al.* 2017, Boonchai *et al.* 2017, Chakeri and Unver 2014, Cui *et al.* 2016, Deb and Das 2014, Do *et al.* 2015, Goh and Mair 2014, Hadi *et al.* 2016, Han *et al.* 2013, Huang *et al.* 2016, Huang *et al.* 2017, Ieronymaki *et al.* 2017, Ibrahim 2014, Iraji and Farzaneh 2016, Lam *et al.* 2014, Maghous *et al.* 2015, Nguyen *et al.* 2015a, b, Pan and Dias 2016, Pinyol and Alonso 2012, Park and Tonavanich 2008, Park and Kim 2006, Park 2014, Lee and Pietruszczak 2008, Ranjbarnia *et al.* 2016, Rao *et al.* 2017, Showkati *et al.* 2016, Shin *et al.* 2012, Talmon and Bezuijen 2013, Ullah *et al.* 2013, Vu *et al.* 2017, Wan *et al.* 2017, Wang *et al.* 2017, Xiao and Liu 2017, Zhang *et al.* 2014, Zhou *et al.* 2016, Zou and Li 2015, Zou and He 2016, Zou and Zuo 2017a, Zou et al. 2018, 2019a, b, c, d, e), few theoretical solutions have been reported in technical literature, especially those for strain-softening surrounding rock.

This study presents a new numerical procedure to calculate the distributions of stresses analytically and displacements numerically for circular opening excavated in strain-softening rock masses with M-C and H-B criteria.

## 2. Theory and methodology

### *2.1 Assumptions*

Several assumptions have been made to determine the distributions of stresses and displacements. A circular opening of radius $b$ is excavated in a continuous, homogeneous, isotropic, initially elastic rock mass, subjected to an initial hydrostatic stress. There is an internal support pressure at the tunnel surface. A plastic zone occurs around the tunnel when pi is less than a critical value. The plastic zone is divided into the softening zone and residual zone. The distributions of stresses and displacements in the plastic region should be solved numerically. The rock masses adhere to M-C and generalized H–B failure criteria under the plane strain condition. The strain-softening constitutive model that follows a non-associated flow rule is employed (as shown in Fig. 1). The elastic strain in the plastic and softening regions of the surrounding rock accords with Hooke's law. When the plastic zone develops, the strength parameters drop gradually. The strength and

∗Corresponding author, Professor
E-mail: zoujinfeng_csu@163.com


http://www.techno-press.org/?journal=gae&subpage=7

ISSN: 2005-307X (Print), 2092-6219 (Online)

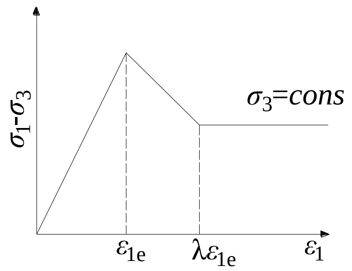


Fig. 1 Strain-softening material behavior model

deformation parameters, as well as the dilation angle of rock mass, deteriorate with the development of plastic deformation after the post-strength surface shrinks. The material parameters of rock masses are determined according to the bilinear function of plastic shear strain. Compressive stress and direct strain are regarded as positive throughout the process.

In Fig. 1, $\sigma_1$ and $\sigma_3$ are the major and minor principal stresses, respectively. $\varepsilon_1$ and $\lambda\varepsilon_1$ are the major principal elastic strain and the component of the maximum principal strain at the interface between the softening and residual regions. $\varepsilon_1$ is the maximum elastic strain.

### 2.2 Evolution of the strength and deformation parameters

The strength and deformation parameters of the strain-softening rock mass are evaluated based on plastic deformation and controlled by the deviatoric shear strain (Alonso *et al.* 2003).

$$\gamma_p = \varepsilon_1^{\mathrm{p}} - \varepsilon_3^{\mathrm{p}} \tag{1}$$

where, $\varepsilon_1^{\mathrm{p}}$ and $\varepsilon_3^{\mathrm{p}}$ are the major and minor plastic strains, respectively.

The physical parameters of the surrounding rock are described according to the bilinear function of plastic shear strain as follows (Alonso *et al.* 2003).

$$\omega\left(\gamma_p\right)=\begin{cases}\omega_{\mathrm{p}}-\left(\omega_{\mathrm{p}}-\omega_{\mathrm{r}}\right)\dfrac{\gamma_p}{\gamma_p^*}, & 0<\gamma_p<\gamma_p^* \\ \omega_{\mathrm{r}} & , \ \gamma_p \ge \gamma_p^*\end{cases}, \tag{2}$$

$$\psi\left(\gamma_p\right)=\begin{cases}\psi_p\text{-}\left(\psi_p\text{-}\psi_r\right)\dfrac{\gamma_p}{\gamma_p^*}, & 0<\gamma_p<\gamma_p^* \\ \psi_r & , \ \gamma_p \ge \gamma_p^*\end{cases}, \tag{3}$$

where, $\omega$ represents a strength parameter, such as $m$, $s$, $c$, $\varphi$, and $\sigma_c$; and $\gamma_p^*$ is the critical deviatoric plastic strain from which the residual behavior is first observed and should be identified through experimentation. The subscripts $p$ and $r$ represent the peak and residual values, respectively. $\psi_p$ and $\psi_4$ are the peak and residual values of the dilation angle of the rock, respectively; $\gamma_p$ is the softening parameter. When $\gamma_p^*=\infty$ and $\gamma_p^*=0$, the elastic-plastic model and elastic-brittle-plastic model are retrieved, respectively.

### 2.3 Failure criterion

The following failure criterion is adopted by

$$F(\sigma_\theta,\sigma_r,\gamma_p)=\sigma_\theta-\sigma_r-H(\sigma_r,\gamma_p) \tag{4}$$

where, $\sigma_\theta$ and $\sigma_r$ are the radial and circumferential principal stresses, respectively.

For H-B failure criterion, $H$ can be expressed as

$$H(\sigma_r,\gamma_p)=\sigma_c(\gamma_p)\left(m(\gamma_p)\frac{\sigma_r}{\sigma_c(\gamma_p)}+s(\gamma_p)\right)^{a(\gamma_p)} \tag{5}$$

where, $\sigma_c$ is the uniaxial compressive strength H-B of rock; $m$, $s$ and $a$ are the strength parameters of H-B criterion.

For M-C failure criterion, $H$ can be expressed as

$$H(\sigma_r,\gamma_p)=(N(\gamma_p)-1)\sigma_r+Y(\gamma_p) \tag{6}$$

where $N$ and $Y$ are strength parameters defined in terms of friction angle $\varphi(\gamma_p)$ and cohesion $c(\gamma_p)$.

$$N(\gamma_p)=\frac{1+\sin(\varphi_p)}{1-\sin(\varphi_p)} \tag{7}$$

$$Y(\gamma_p)=\frac{2c(\gamma_p)\cos(\varphi_p)}{1-\sin(\varphi_p)} \tag{8}$$

### 2.4 Critical supporting pressure

When the internal supporting pressure is less than critical value $p_{ic}$, the plastic region occurs . For M-C and H-B rock masses, $p_{ic}$ can be calculated (Kennedy and Lindberg 1978), respectively, as follows

$$p_{ic}^{M-C}=\frac{2p_0-Y_p}{N_p+1} \tag{9}$$

$$2\left(\sigma_0-p_{ic}\right)=\sigma_{cp}\left(m_p\frac{p_{ic}}{\sigma_{cp}}+s_p\right)^{a_p} \tag{10}$$

when $a_p$=0.5, the analytical solution of $p_{ic}$ can be expressed as

$$p_{ic}^{H-B}=\frac{1}{2}\left(\beta-\sqrt{\beta^2+4\beta p_0+s_p\sigma_{cp}^2}\right)+p_0 \tag{11}$$

where $Y_p=2c_p\cos\varphi_p/(1-\sin\varphi_p)$, $N_p=(1+\sin\varphi_p)/(1-\sin\varphi_p)$, and $\beta=(m_p\sigma_{cp})/4$. When $a_p$ ≠0.5, the solution of $p_{ic}$ can be found numerically by using Newton-Raphson method.

### 2.5 Flow rule

The non-associated flow rule is used for determination of plastic strain. The relation between the radial and circumferential plastic strain increments can be expressed as

$$d\varepsilon_r^p = -k(\gamma_p) d\varepsilon_\theta^p \tag{12}$$

where, $k(\gamma_p)$ is known as the coefficient of dilation and can be expressed as

$$k(\gamma_p) = \frac{1+\sin\psi(\gamma_p)}{1-\sin\psi(\gamma_p)} \tag{13}$$

If $k(\gamma_p) = 1$, no plastic volume change takes place when the plastic region develops.

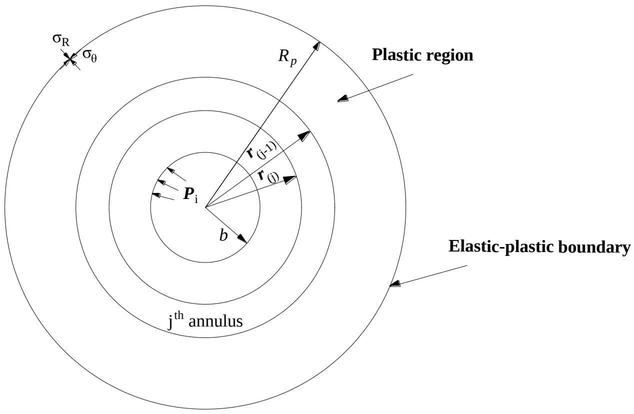


Fig. 2 Plastic region with a finite number of annuli

## 3. Solutions of stress and displacement

### *3.1 Determination of plastic region*

Unlike other numerical approaches, in this study, radial-increment-approach and stress solving technique are similar to the approach in Zou *et al.* (2017), while the total strain and displacement for each annulus can be obtained by finite difference method for each concentric annuls. The elastic strain increment can be calculated by use of Hooke's law. Combining the plastic flow rule, the plastic strain increment, $\varepsilon_{\theta(i)}^p$ and $\varepsilon_{r(i)}^p$, can be given by approximating the compatibility equation. Thus the total strain and displacement for each annulus can be obtained by finite difference method.

### *3.2 Increments of stress and strain*

As shown in Fig. 2, the plastic zone is divided into concentric rings by radius. The increment of radius $\Delta r$, the inner radii of each annulus and the radial stress with M-C, H-B and general H-B failure criteria can be expressed, respectively, as follows (Zou *et al.* 2017).

$$\Delta r = \frac{b-R_p}{n} \tag{14}$$

$$r_{(j)} = r_{(j-1)} + \Delta r \tag{15}$$

$$\sigma_{r(j)} = \frac{m_{r(j)}\sigma_{c(j)}}{4}\left[\ln\left(\frac{r_{(j)}}{r_{(j-1)}}\right)\right]^2 + \left[\ln\left(\frac{r_{(j)}}{r_{(j-1)}}\right)\right]\sqrt{m_{r(j)}\sigma_{c(j)}\sigma_{r(j-1)} + s_{r(j)}\sigma_{c(j)}^2} + \sigma_{r(j-1)} \tag{16}$$

$$\sigma_{r(j)} = \frac{[(A\sigma_{r(j-1)} + s_{r(j-1)})^B + Am_{r(j-1)}\ln(r_{(j)}/r_{(j-1)})]^{1/B} - s_{r(j-1)}}{A} \tag{17}$$

$$\sigma_{r(j)} = \frac{Y_{(j)}}{1-N_{(j)}} + \left(\frac{Y_{(j)}}{1-N_{(j)}} + \sigma_{r(j-1)}\right)\frac{r_{(j-1)}}{r_{(j)}} \tag{18}$$

where, $A = \dfrac{m_{r(j-1)}}{\sigma_{c(j-1)}}$ and $B = 1 - a_{r(j-1)}$.

From Eqs. (16), (17) or (18), the radial stress increment at the *j*th annulus can be obtained as follows

$$\Delta\sigma_{r(j)} = \sigma_{r(j)} - \sigma_{r(j-1)} \tag{19}$$

It should be noted that the initial radial stress equals the critical supporting pressure, $\sigma_{(0)} = p_{ic}$. Thus,

$$\sigma_{\theta(j)} = \sigma_{r(j)} + H(\sigma_{r(j)}, \gamma_{(j-1)}^p) \tag{20}$$

Then the circumferential stress increment can be stated as

$$\Delta\sigma_{\theta(j)} = \sigma_{\theta(j)} - \sigma_{\theta(j-1)} \tag{21}$$

In order to calculate the strain increments and displacements, the strain-displacement relation and compatibility equation are given by

$$\varepsilon_r = \frac{du}{dr}, \varepsilon_\theta = \frac{u}{r} \tag{22}$$

$$\frac{d\varepsilon_\theta^p}{dr} + \frac{\varepsilon_\theta - \varepsilon_r}{r} = 0 \tag{23}$$

The strain components consist of elastic and plastic parts as follows.

$$\begin{Bmatrix}\varepsilon_\theta \\ \varepsilon_r\end{Bmatrix} = \begin{Bmatrix}\varepsilon_\theta^e \\ \varepsilon_r^e\end{Bmatrix} + \begin{Bmatrix}\varepsilon_\theta^p \\ \varepsilon_r^p\end{Bmatrix} \tag{24}$$

So that equation (24) can be rewritten as

$$\frac{d\varepsilon_\theta^p}{dr} + \frac{\varepsilon_\theta^p - \varepsilon_r^p}{r} = -\frac{d\varepsilon_\theta^e}{dr} - \frac{\varepsilon_\theta^e - \varepsilon_r^e}{r} \tag{25}$$

or

$$\frac{d\varepsilon_\theta^p}{dr} + \frac{\varepsilon_\theta^p - \varepsilon_r^p}{r} = -\frac{d\varepsilon_\theta^e}{dr} - \frac{(1+v)}{E}\frac{H(\sigma_r, \gamma^p)}{r} \tag{26}$$

Approximating the differential Eq. (26) and using Eqs. (11) and (12), the following equation can be obtained.

$$\Delta\varepsilon_{\theta(j)}^p\left(\frac{1}{\Delta r} + (1-k_{(j-1)})\frac{1}{\bar{r}_{(j)}}\right) = -\frac{\Delta\varepsilon_{\theta(j)}^e}{\Delta r} - \frac{(1+v)}{E}\frac{H(\sigma_{r(j)}, \gamma_{(j-1)}^p)}{\bar{r}_{(j)}} - \frac{1}{\bar{r}_{(j)}}(\varepsilon_{\theta(j-1)}^p - \varepsilon_{r(j-1)}^p) \tag{27}$$

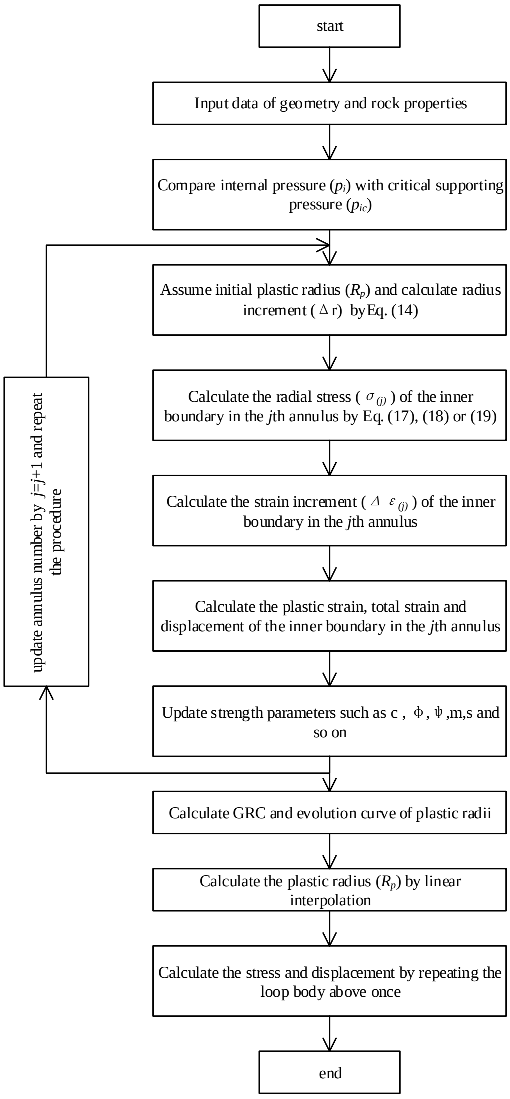

Fig. 3 Flow chart of the sequence of calculations

where, $\bar{r}_{(j)} = (r_{(j)} + r_{(j-1)})/2$, and $k_{(j-1)} = (1+\sin\psi_{(j-1)})/(1-\sin\psi_{(j-1)})$. Using Hooke's law, $\Delta\varepsilon^e_{r(j)}$ and $\Delta\varepsilon^e_{\theta(j)}$ can be given by

$$\begin{Bmatrix} \Delta\varepsilon^e_{r(j)} \\ \Delta\varepsilon^e_{\theta(j)} \end{Bmatrix} = \frac{1+\nu}{E} \begin{bmatrix} 1-\nu & -\nu \\ -\nu & 1-\nu \end{bmatrix} \begin{Bmatrix} \Delta\sigma_{r(j)} \\ \Delta\sigma_{\theta(j)} \end{Bmatrix} \tag{28}$$

Corresponding $\Delta\varepsilon^p_{r(j)}$ is then given by Eq. (12). The softening parameter can be updated as

$$\gamma^p_{(j)} = \gamma^p_{(j-1)} + \left(\Delta\varepsilon^p_{\theta(j)} - \Delta\varepsilon^p_{r(j)}\right) \tag{29}$$

Then the total strain at $j$th annulus is obtained as

$$\begin{Bmatrix} \varepsilon_{r(j)} \\ \varepsilon_{\theta(j)} \end{Bmatrix} = \begin{Bmatrix} \varepsilon_{r(j-1)} \\ \varepsilon_{\theta(j-1)} \end{Bmatrix} + \begin{Bmatrix} \Delta\varepsilon^e_{r(j)} \\ \Delta\varepsilon^e_{\theta(j)} \end{Bmatrix} + \begin{Bmatrix} \Delta\varepsilon^p_{r(j)} \\ \Delta\varepsilon^p_{\theta(j)} \end{Bmatrix} \tag{30}$$

Using strain-displacement relation, the displacement at *r(j)* can be

$$u_{(j)} = \varepsilon_{\theta(j)} r_{(j)} \tag{31}$$

Step by step, all displacements and stresses in plastic annuli can be obtained from the outmost annulus to the innermost one with the boundary conditions: $\sigma_{r(n)} = p_i$ and $u_{(n)} = u_0$. GRC can be obtained by combining Eqs. (20) and (32), and the real plastic radius can be found by using linear interpolation. The flow chart for the sequence of the proposed approach is shown in Fig. 3.

## 4. Verification and application

### *4.1 Verification*

In order to validate the proposed approach, results with the proposed approach and those in Brown *et al.* (1983), Park *et al.* (2008) and Lee and Pietruszczak (2008) are compared (as shown in Fig. 4.). The rock properties appearing in Lee and Pietruszczak (2008) are as follows: $b$=3 m, $E$=5700 MPa, $\nu$=0.25, $\sigma_{cp}$=30 MPa, $\sigma_{cr}$=25 MPa,

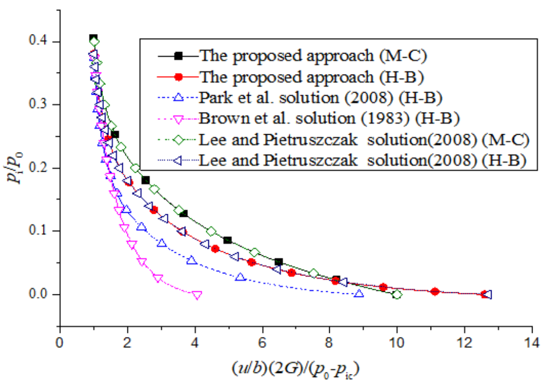


(a) For H-B and M-C criteria

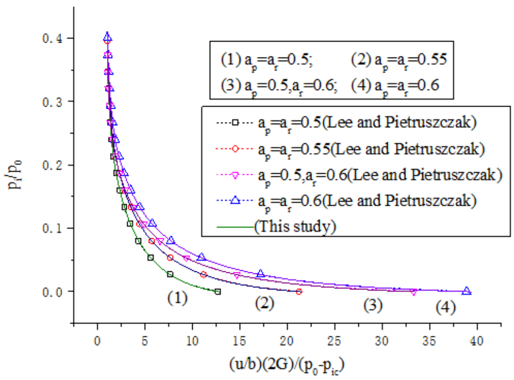


(b) For generalized H-B criterion

Fig. 4 GRC using different approaches for different failure criteria

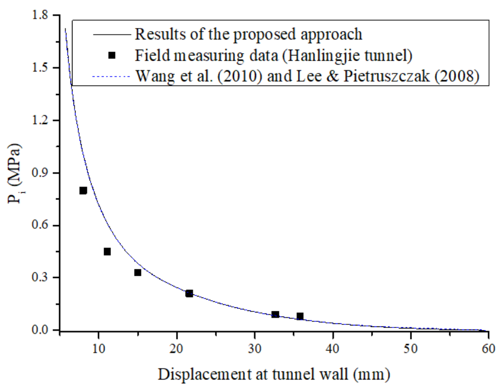


Fig. 5 Convergence-confinement curve with field measuring data

$p_0$=15 MPa, $m_p$=2.0, $m_r$=0.6, $s_p$=0.004, $s_r$=0.002, $a_p$=0.5, $a_r$=0.5, $\psi_p$=15°, $\psi_r$=5°, $\gamma_p^*$=0.01. To compare the results based on the generalized H-B and M-C failure criterion, the technique of equivalent M-C and generalized H-B strength parameters was adopted and the equations for the friction angle ($\phi$) and cohesive ($c$) are given by Hoek *et al.* (2002). Then, for M-C failure criterion, the strength parameters are as follows: $c_p$=2.52 MPa, $\varphi_p$=26.36°, $c_r$=1.52 MPa, $\varphi_r$=16.57°.

GRCs are illustrated for M-C and H-B failure criteria in Fig. 4, respectively. It can be seen from Fig. 4 that the results of the proposed approach are in well agreement with those of Lee and Pietruszczak (2008). For H-B failure criterion, the displacements in Park *et al.* (2008) and Brown *et al.* (1983), $(u/b)(2G)/(p_0-p_{ic})$, are respectively 29.5% and 67.5% lower than that of the proposed approach; the displacement in Lee and Pietruszczak (2008) 0.9% lager than that in the proposed procedure when the internal supporting pressure $p_i$=0.

For M-C failure criterion, the displacement at the tunnel wall are 20.6% lower than that for H-B failure criterion by using the equivalent parameter values as the internal supporting pressure is 0. Meanwhile, the displacements in this study and Lee and Pietruszczak (2008) are the same value, 9.99. For generalized H-B failure criterion, the results in Fig. 4(b) are in agreement with those in Lee and Pietruszczak (2008). When $a_p$=$a_r$=0.5, the generalized H-B failure criterion becomes H-B failure criterion and the same results are shown in Fig. 4(a).

### *4.2 Application of design*

To confirm the validity and accuracy of the proposed approach, the results of the proposed approach and field measuring data in Hanlingjie tunnel are compared. Basic information of Hanlingjie tunnel can be seen in Zou *et al.* (2017). According to the geological investigation, laboratory experiments and inverse calculation, the basic parameters of surrounding rock are obtained by the local test and shown as follows: $b$=5.5 m, $E$=4 GPa, $v$=0.35, $p_0$=4.8 MPa, $\sigma_{cp}$=10 MPa, $\sigma_{ce}$=6 MPa, $m_p$=2.23, $s_p$=0.0013, $a_p$=0.51, $m_r$=0.86, $s_r$=0.0002, $a_r$=0.52, $\psi_p$=13°, $\psi_r$=5°, $\gamma_p^*$=0.008. Based on these parameters, the convergence-confinement results of the proposed approach and field measurement data are shown in Fig. 5. It can be observed that the results in the proposed approach and Lee and Pietruszczak (2008) are basically consistent with field measurement data.

## 5. Numerical calculation and discussion

### *5.1 Influence of annulus number n*

(1) For H-B criterion

To investigate the influence of annulus number n on the results of the proposed approach, an elastic-brittle-plastic analysis is performed. In this analysis, the closed solutions in Park and Kim (2006) are compared to the results of the proposed approach. The rock properties appearing in Park and Kim (2006) are taken as input data: $b$=5 m, $p_0$=30 MPa, $p_i$=5 MPa, $E$=5 GPa, $v$=0.25, $\sigma_{cp}$=$\sigma_{cr}$=30 MPa, $m_p$=1.7, $s_p$=0.0039, $m_r$=1.0, $S_r$=0.0. Two dilation angles, $\psi$=0° and $\psi$=30°, are adopted to investigate the effect of plastic volume change. Since the differences is slight, three different annulus numbers, n=20, 100 and 500, are considered in both situations. The results are shown in Figs. 6 and 7.

It can be seen from Fig. 6 that the larger annulus number $n$ is, the more accurate the solutions are; and the maximum displacement difference occurs on the excavation surface, $r/b$=1. When $\psi$=0°, for $n$=500 the difference is 0.25%. When $\psi$=30°, for $n$=500 the difference is 0.70%. This indicates that the dilation angle lowers the accuracy of the displacement.

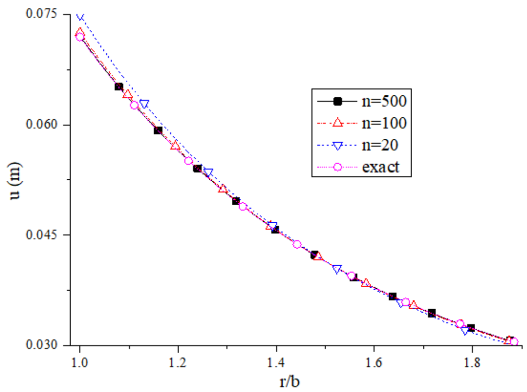


(a) $\psi=0^{\circ}$

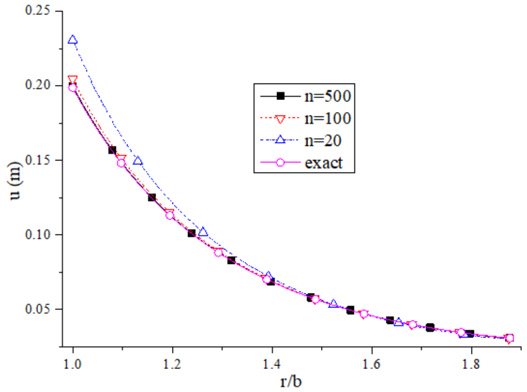


(b) $\psi=30^{\circ}$

Fig. 6 Displacements for different annulus number n in M-C rock mass

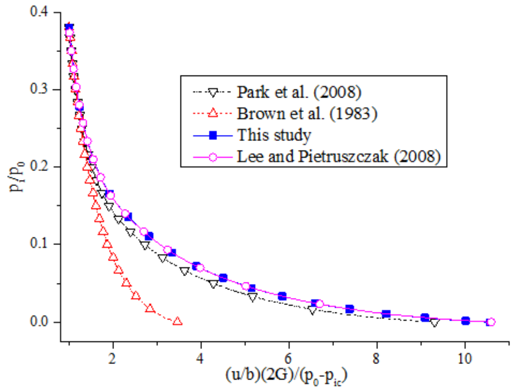


(a) $\psi_p=\psi_r=5^{\circ}$

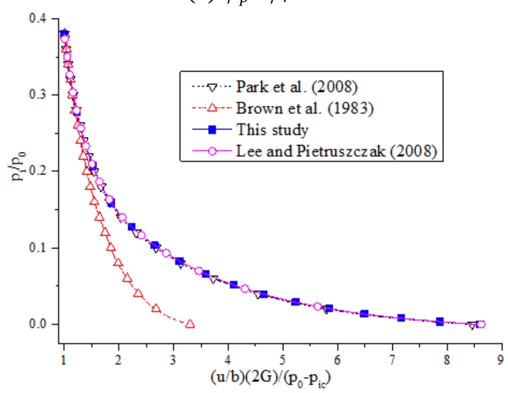


(b) $\psi_p=\psi_r=0^{\circ}$

Fig. 8 GRC for different procedures using different dilation angles

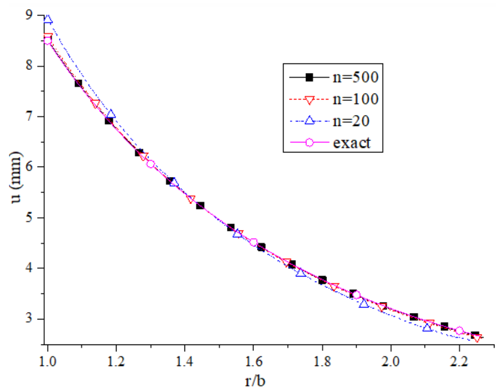


(a) $\psi=0^{\circ}$

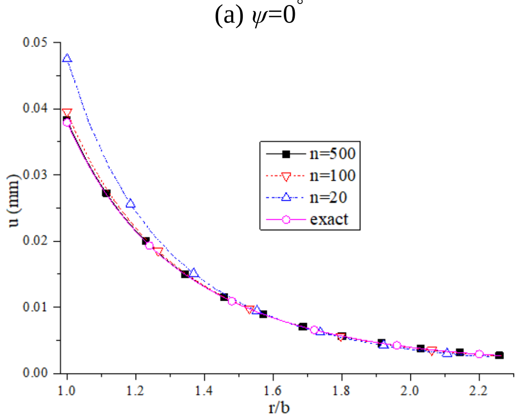


(b) $\psi=30^{\circ}$

Fig. 7 Displacements for different annulus number n in H-B rock mass

(2) For M-C criterion

To investigate the influence of annulus number $n$ for M-C criterion, a set of data appearing in Lee and Pietruszczak (2008) are employed as input data. The data are $b$ =5 m, $p_0$=3 MPa, $p_i$=0 MPa, $E$=10 GPa, $\upsilon$=0.2, $\varphi_p$=30°, $\varphi_r$=26°, $c_p$=0.5 MPa, $c_r$=0.2 MPa. The same as H-B rock mass, two dilation angles, $\psi$=0° and $\psi$=30°, are adopted to study the effect of the plastic volume change. Three annulus numbers, $n$ = 20, 100 and 500, are applied here for both conditions. The results are shown in Fig. 7.

It can see form Fig. 7 that the annulus number $n$ has larger effect on the displacements in the plastic region when the rock mass is more dilatant. When $\psi$=0°, for $n$=500 the maximum difference is 0.31%. When $\psi$=30°, for $n$=500 the maximum difference is 1.03%. This means that the calculated displacements are close enough to exact ones.

### *5.2 Influence of dilation on GRC between different approaches*

There are several studies for the strain softening model in Hoek-Brown rock mass, including Brown *et al.* (1983), Lee and Pietruszczak (2008), and Park *et al.* (2008). Dilation is a significant factor influencing the results of the proposed procedures. Therefore, the GRC in this studies are compared using different dilation angles. A set of data in Section 4.1 are employed. But two sets of dilation angles are adopted here: (1) $\psi_p=\psi_r=5^{\circ}$, (2) $\psi_p=\psi_r=0^{\circ}$. The results are shown in Fig. 8.

Fig. 8 shows that the results of the proposed approach are in well agreement with those in Lee and Pietruszczak (2008). When $\psi_p=\psi_r=5^\circ$, the displacements in Park *et al.* (2008) and Brown *et al.* (1983) are 11.9% and 67.2%, respectively, lower than the displacement in this study as $p_i=0$. The displacement in Lee and Pietruszczak (2008) is 0.2% larger than the displacement in this study as $p_i=0$. When $\psi_p=\psi_r=0^\circ$, the displacements in Park *et al.* (2008) and Brown *et al.* (1983) and are 1.6% and 61.6%, respectively, lower than the displacement in this study as $p_i=0$. The displacement in Lee and Pietruszczak (2008) is 0.2% larger than the displacement in this study as $p_i=0$. It should be noted that when $\psi_p=15^\circ$ and $\psi_r=5^\circ$ in Section 4.1, the difference between the displacements in Park *et al.* (2008) and this study is 29.5%. When $\psi_p=\psi_r=5^\circ$, the difference decreases into 11.9%. When $\psi_p=\psi_r=0^\circ$, the difference decreases into 1.6%. While the differences of the solutions between Brown *et al.* (1983), Lee and Pietruszczak (2008) and this study are relatively stable. It can be summarized that the dilation has a significant influence on Park *et al.* (2008) solutions.

### *5.3 Discussion on the calculation efficiency*

The proposed procedure is programmed into a Matlab code. When the code is executed on a desktop computer with Core i5 CPU of 3.1 GHz clock speed, the runtime required to get each solution(displacement) presented in Section 5.1 is only 14.4 ms for n=500. Whereas, Lee and Pietruszczak (2008) spends 15.3 ms when applying their approach by using the same parameters. We can see that the procedure in this study is 6% faster than Lee and Pietrucszczak's (2008). The difference lies in the different stress computation speed though the approach of this study and Lee and Pietruszczak (2008) use the same means to obtain the strain. The procedure in this study obtains the analytical stress solutions. However, Lee and Pietrucszczak (2008) used the finite difference method to get stress solutions. The proposed procedure is also 8% faster than that in Lee and Piertruszczak(2008) when calculating GRC. Nevertheless, it is more complex to obtain the plastic radius using the proposed procedure. Due to the extensive application of GRC, the complicacy is acceptable and the proposed procedure is rather economical.

## 6. Conclusions

A new numerical procedure is proposed for calculating the stresses and displacements of a circular opening. In the proposed procedure, the plastic region is divided into a finite number of concentric annuli, whose thickness is uniformly determined by a small radius increment. The stresses for each annulus can be obtained analytically. The strain increments for each annulus can be calculated numerically from the finite difference approximation of the compatility equation by invoking the flow rule and Hooke's law. By assuming different plastic radii, GRC and the evolution curve of plastic radii and internal supporting pressures can be obtained conveniently. Then the real plastic radius can be calculated by using linear interpolation in the evolution curve.

Some numerical and engineering examples are performed to demonstrate the accuracy and validity of the proposed procedure.

## Acknowledgements

This work was supported by the National Key R&D Program of China (2017YFB1201204), the National Natural Science Foundation of China (Grant No. 51478478).

## References

Alessandra, P., Schweiger, H.F. and Giuseppe, S. (2017), "Numerical analyses of stability and deformation behavior of reinforced and unreinforced tunnel faces", *Comput. Geotech.*, **88**, 256-266.

Alonso, E., Alejano, L.R., Varas, F., Fdez-Manin, G. and Carranza-Torres, C. (2003), "Ground response curves for rock masses exhibiting strain-softening behaviour", *Int. J. Numer. Anal. Meth. Geomech.*, **27**(3), 1153-1185.

Apostolos, V. (2017), "A finite strain solution for the elastoplastic ground response curve in tunnelling: Rocks with non-linear failure envelopes", *Int. J. Numer. Anal. Meth. Geomech.*, **41**(3), 1077-1090.

Boonchai, U., Kongkit, Y. and Suraparb, K. (2017), "Three-dimensional undrained tunnel face stability in clay with a linearly increasing shear strength with depth", *Comput. Geotech.*, **88**(8), 146-151.

Chakeri, H. and Unver, B. (2014), "A new equation for estimating the maximum surface settlement above tunnels excavated in soft ground", *Environ. Earth Sci.*, **71**(7), 3195-3210.

Cui, Q.L., Wu, H.N., Shen, S.L., Yin, Z.Y. and Horpibulsuk, S. (2016), "Protection of neighbour buildings due to construction of shield tunnel in mixed ground with sand over weathered granite", *Environ. Earth Sci.*, **75**(6), 458.

Deb, D. and Das, K.C. (2014), "A new doubly enriched finite element for modelling grouted bolt crossed by rock joint", *Int. J. Rock Mech. Min. Sci.*, **70**(9), 47-58.

Do, N.A., Dias, D. and Oreste, P. (2015), "3D numerical investigation on the interaction between mechanized twin tunnels in soft ground", *Environ. Earth Sci.*, **73**(5), 2101-2113.

Fahimifar, A. and Ranjbarnia, M. (2011), "Analysis of circular reinforced tunnels by analytical approach", *J. Struct. Eng. Geotech.*, **1**(2), 45-55.

Fahimifar, A. and Zareifard, M.R. (2009), "A theoretical solution for analysis of tunnels below groundwater considering the hydraulic-mechanical coupling", *Tunn. Undergr. Sp. Technol.*, **24**(6), 634-646.

Fahimifar, A. and Zareifard, M.R. (2013), "A new closed-form solution for analysis of unlined pressure tunnels under seepage forces", *Int. J. Numer. Anal. Meth. Geomech.*, **37**(11), 1591-1613.

Farhadian, H., Katibeh, H. and Huggenberger, P. (2016), "Empirical model for estimating groundwater flow into tunnel in discontinuous rock masses", *Environ. Earth Sci.*, **75**(6), 471.

Goh, K.H. and Mair, R.J. (2014), "Response of framed buildings to excavation-induced movements", *Soil. Found.*, **54**(3), 250-268.

Han, J.X., Li, S.C., Li, S.C. and Yang, W.M. (2013), "A procedure of strain-softening model for elasto-plastic analysis of a circular opening considering elasto-plastic coupling", *Tunn. Undergr. Sp. Technol.*, **37**, 128-134.

Huang, F., Zhu, H., Jiang, S. and Liang, B. (2016), "Excavation-damaged zone around tunnel surface under different release ratios of displacement", *Int. J. Geomech.*, **17**(4), 04016094.

Ibrahim, O. (2014), "A new approach for estimating the transverse surface settlement curve for twin tunnels in shallow and soft soils", *Environ. Earth Sci.*, **72**(7), 2357-2367.

Ieronymaki, E.S., Whittle, A.J. and Sureda, D.S. (2017), "Interpretation of free-field ground movements caused by mechanized tunnel construction", *J. Geotech. Geoenviron. Eng.*, **143**(4), 04016114.

Iraji, A. and Farzaneh, O. (2016), "Two-phase model for nonlinear dynamic simulation of reinforced soil walls based on a modified pastor-Zienkiewicz-Chan model for granular soil", *J. Eng. Mech.*, **142**(2), 04015072.

Lam, S.Y., Haigh, S.K. and Bolton, M.D. (2014), "Understanding ground deformation mechanisms for multi-propped excavation in soft clay", *Soil. Found.*, **54**(3), 296-312.

Lee, Y.K. and Pietruszczak, S. (2008), "A new numerical procedure for elasto-plastic analysis of a circular opening excavated in a strain-softening rock mass", *Tunn. Undergr. Sp. Technol.*, **23**(5), 588-599.

Maghous, S., Winiawer, J.E.B. and Pasa Dutra, V.F. (2015), "Stability analysis of tunnels driven in jointed rocks by means of a homogenized limit analysis approach", *Int. J. Numer. Anal. Meth. Geomech.*, **38**(18), 2009-2032.

Nguyen, T., Ghabraie, K. and Tran-Cong, T. (2015), "Simultaneous pattern and size optimisation of rock bolts for underground excavations", *Comput. Geotech.*, **66**, 264-277.

Nguyen, T., Ghabraie, K., Tran-Cong, T. and Fatahi, B. (2015), "Improving rockbolt design in tunnels using topology optimization", *Int. J. Geomech.*, **16**(1), 04015023.

Pan, Q. and Dias, D. (2016), "The effect of pore water pressure on tunnel face stability", *Int. J. Numer. Anal. Meth. Geomech.*, **40**(15), 2123-2136.

Park, K.H. (2014), "Similarity solution for a spherical or circular opening in elastic-strain softening rock mass", *Int. J. Rock Mech. Min. Sci.*, **71**, 151-159.

Park, K.H. and Kim, Y.J. (2006), "Analytical solution for a circular opening in an elastic-brittle-plastic rock", *Int. J. Rock Mech. Min. Sci.*, **43**(4), 616-622.

Park, K.H., Tonavanich, B. and Lee, J.G. (2008), "A simple procedure for ground response curve of circular tunnel in elastic-strain softening rock mass", *Tunn. Undergr. Sp. Technol.*, **23**(2), 151-159.

Pinyol, N.M. and Alonso, E.E. (2012), "Design of micropiles for tunnel face reinforcement: Undrained upper bound solution", *J. Geotech. Geoenviron. Eng.*, **138**(1), 89-99.

Ranjbarnia, M., Oreste, P., Fahimifar, A. and Arya, A. (2016), "Analytical-numerical solution for stress distribution around tunnel reinforced by radial fully grouted rockbolts", *Int. J. Numer. Anal. Meth. Geomech.*, **40**(13), 1844-1862.

Rao, P.P., Chen, Q.S., Li, L., Nimbalkar, S. and Cui, J.F. (2017), "Elastoplastic solution for spherical cavity expansion in modified Cam-Clay soil under drained condition", *Int. J. Geomech.*, **17**(8), 06017005.

Shin, J.H., Kim, S.H. and Shin, Y.S. (2012), "Long-term mechanical and hydraulic interaction and leakage evaluation of segmented tunnels", *Soil. Found.*, **52**(1), 38-48.

Showkati, A., Maarefvand, P. and Hassani, H. (2015), "An analytical solution for stresses induced by a post-tensioned anchor in rocks containing two perpendicular joint sets", *Acta Geotechnica*, **11**(2), 415-432.

Showkati, A., Maarefvand, P. and Hassani, H. (2016), "An analytical solution for stresses induced by a post-tensioned anchor in rocks containing two perpendicular joint sets", *Acta Geotechnica*, **11**(2), 415-432.

Talmon, A.M. and Bezuijen, A. (2013), "Analytical model for the beam action of a tunnel lining during construction", *Int. J. Numer. Anal. Meth. Geomech.*, **37**(2), 181-200.

Tang, X.W., Liu, W., Albers, B. and Savidis, S. (2014), "Upper bound analysis of tunnel face stability in layered soils", *Acta Geotechnica*, **9**(4), 661-671.

Ullah, S., Pichler, B. and Hellmich, C. (2013), "Modeling ground-shell contact forces in NATM tunneling, based on 3D displacement measurements", *J. Geotech. Geoenviron. Eng.*, **139**(3), 444-457.

Vu, M.N., Broere, W. and Bosch, J.W. (2017), "Structural analysis for shallow tunnels in soft soils", *Int. J. Geomech.*, 04017038.

Wan, M.S.P., Standing, J.R., Potts, D.M. and Burland, J.B. (2017), "Measured short-term ground surface response to EPBM tunnelling in London clay", *Géotechnique*, **67**(5), 420-445.

Wang, H.N., Zeng, G.S., Utilic, S., Jiang, M.J. and Wu, L. (2017), "Analytical solutions of stresses and displacements for deeply buried twin tunnels in viscoelastic rock", *Int. J. Rock Mech. Min. Sci.*, **93**(3), 13-29.

Xiao, Y. and Liu, G.B. (2017), "Performance of a large-scale metro interchange station excavation in Shanghai soft clay", *J. Geotech. Geoenviron. Eng.*, **143**(6), 05017003.

Zhang, D.M., Huang, H.W., Phoon, K.K. and Hu, Q.F. (2014), "A modified solution of radial subgrade modulus for a circular tunnel in elastic ground", *Soil. Found.*, **54**(2), 225-232.

Zhou, H., Xiao, M. and Chen, J. (2016), "Analysis of a numerical simulation method of fully grouted and anti-seismic support bolts in underground geotechnical engineering", *Comput. Geotech.*, **76**, 61-74.

Zou, J.F., Wei, A. and Yang, T. (2018), "Elasto-plastic solution for shallow tunnel in semi-infinite space", *Appl. Math. Model.*, **64**(12), 669-687.

Zou, J.F. and He, Z. (2016), "Numerical approach for strain-softening rock with axial stress", *Proc. Inst. Civ. Eng. Geotech. Eng.*, **169**(3), 276-290.

Zou, J.F. and Li, S.S. (2015), "Theoretical solution for displacement and stress in strain-softening surrounding rock under hydraulic-mechanical coupling", *Sci. China Technol. Sci.*, **58**(8), 1401-1413.

Zou, J.F. and Zou, S.Q. (2017a), "Similarity solution for the synchronous grouting of shield tunnels under the non-axisymmetric displacement boundary on vertical surface", *Adv. Appl. Math. Mech.*, **9**(1), 205-232.

Zou, J.F., Li, C. and Wang, F. (2017b), "A new procedure for ground response curve (GRC) in strain-softening surrounding rock", *Comput. Geotech.*, **89**, 81-91.

Zou, J.F. and Zhang, P.H. (2019a), "Analytical model of fully grouted bolts in pull-out tests and in situ rock masses", *Int. J. Rock Mech. Min. Sci.*, **113**, 278-294.

Zou, J.F., Chen, G.H. and Qian, Z.H. (2019b), "Tunnel face stability in cohesion-frictional soils considering the soil arching effect", *Comput. Geotech.*, **106**, 1-17.

Zou, J.F., Liu, L. and Xia, M.Y. (2019c), "A new simple approach for the quasi-plane strain problem of circular tunnel in strain-softening rock mass incorporating the effect of out-of-plane stress", *Acta Geotechnica*, In Press.

Zou, J.F., Qian, Z.H., Xiang, X.H. and Chen, G.H. (2019d), "Face stability analysis of tunnel excavated in saturated-nonhomogeneous soil", *Tunn. Undergr. Sp. Technol.*, **83**, 1-17.

Zou, J.F., Wang F. and Wei, A. (2019e), "A semi-analytical solution for shallow tunnels with radius-iterative-approach in semi-infinite space", *Appl. Math. Model.*, In Press.


*CC*